

# Mimicking the Active Center of Methane-monooxygenase by Metal–Peptide Complexes Immobilized on Mesoporous Silica

Lukas Frunz, Roel Prins, and Gerhard D. Pirngruber\*<sup>†</sup>

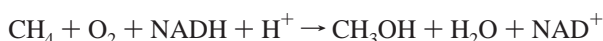
*Institute for Chemical and Bioengineering, ETH Zurich, CH-8093 Zurich, Switzerland*

*Received March 12, 2007. Revised Manuscript Received May 21, 2007*

The short peptide sequence His-Gly-Gly-Glu, which is found in the active center of methane-monooxygenase, was immobilized on a mesoporous silica support. Self-assembled complexes of the peptide with iron and copper cations were allowed to form. Two methods were used to immobilize the peptide on the support. The peptide was either prepared on a solid-phase peptide synthesizer and then grafted on the silica support, or the peptide chain was grown directly on the silica support by a manual step-by-step synthesis. The latter method allowed us to immobilize more peptide on the support, but similar complexes were formed in both methods. Characterization by UV–vis and EXAFS showed that the Cu<sup>2+</sup> cations were coordinated by two histidine residues originating from neighboring peptide chains and additional N/O ligands from the peptide. The complexes were tested in the oxidation of cyclohexane by H<sub>2</sub>O<sub>2</sub>. Activity and selectivity were modest, but higher than those of immobilized metal complexes with single amino acids.

## Introduction

Understanding and copying the catalytic function of metalloproteins is a topic that has fascinated chemists for many years. Many efforts have been made to mimic nature's metalloproteins by synthetic compounds. The synthetic materials help to identify the structural features of the natural enzymes that are crucial for their catalytic action. Second, a more practical point of view, the goal is to develop biomimetic catalysts, which are, like the enzymes, more active and more selective than conventional man-made catalysts. A popular target enzyme is methane-monooxygenase (MMO), which oxidizes methane to methanol according to



The active center of the enzyme is a diiron (or dicopper) core. The iron (or copper) atoms are connected via two carboxylate bridges (acetate and glutamate) and one  $\mu$ -OH bridge. The remaining ligands in the octahedral coordination sphere are two histidine residues, three monodentate glutamic acid residues and water. Both histidine residues and two of the glutamic acid ligands originate from His-Gly-Gly-Glu sequences on the two  $\alpha$ -subunits of the enzyme. Several strategies have been developed to mimic MMO. Bioinorganic chemists have focused on reproducing the active iron core of MMO. Model compounds were prepared, which contain an oxygen-bridged diiron core and ligands similar to MMO.<sup>1–22</sup> The syntheses are difficult because the complexes

are rather reactive<sup>23</sup> and tend to dimerize.<sup>24</sup> The dimerization can be avoided by the use of very bulky ligands.<sup>17,25</sup> Yet, it remains difficult to find a solvent in which the complex, the

- (2) Kitajima, N.; Fukui, H.; Morooka, Y. *J. Chem. Soc., Chem. Commun.* **1988**, 485.
- (3) Rabion, A.; Buchanan, R. M.; Seris, J. L.; Fish, R. H. *J. Mol. Catal. A: Chem.* **1997**, *116*, 43.
- (4) Fish, R. H.; Neumann, R.; Neimann, K.; Rabion, A. *Abstr. Paper Am. Chem. Soc.* **2003**, *226*, 571.
- (5) Buchanan, R. M.; Chen, S.; Richardson, J. F.; Bressan, M.; Forti, L.; Morvillo, A.; Fish, R. H. *Inorg. Chem.* **1994**, *33*, 3208.
- (6) Fish, R. H.; Konings, M. S.; Oberhausen, K. J.; Fong, R. H.; Yu, W. M.; Christou, G.; Vincent, J. B.; Coggin, D. K.; Buchanan, R. M. *Inorg. Chem.* **1991**, *30*, 3002.
- (7) Mekmouche, Y.; Duboc-Toia, C.; Menage, S.; Lambeaux, C.; Fontecave, M. *J. Mol. Catal. A: Chem.* **2000**, *156*, 85.
- (8) Mekmouche, Y.; Menage, S.; Toia-Duboc, C.; Fontecave, M.; Galey, J. B.; Lebrun, C.; Pecaut, J. *Angew. Chem., Int. Ed.* **2001**, *40*, 949.
- (9) Menage, S.; Galey, J. B.; Hussler, G.; Seite, M.; Fontecave, M. *Angew. Chem., Int. Ed.* **1996**, *35*, 2353.
- (10) Menage, S.; Vincent, J. M.; Lambeaux, C.; Fontecave, M. *J. Mol. Catal. A: Chem.* **1996**, *113*, 61.
- (11) Menage, S.; Galey, J. B.; Dumats, J.; Hussler, G.; Seite, M.; Luneau, I. G.; Chottard, G.; Fontecave, M. *J. Am. Chem. Soc.* **1998**, *120*, 13370.
- (12) Menage, S.; Galey, J. B.; Hussler, G.; Seite, M.; Dumats, J.; Gautier-Luneau, I.; Chottard, G.; Fontecave, M. *J. Inorg. Biochem.* **1999**, *74*, 231.
- (13) Menage, S.; Vincent, J. M.; Lambeaux, C.; Chottard, G.; Grand, A.; Fontecave, M. *Inorg. Chem.* **1993**, *32*, 4766.
- (14) Costas, M.; Chen, K.; Que, L. *Coord. Chem. Rev.* **2000**, *200*, 517.
- (15) Jensen, M. P.; Lange, S. J.; Mehn, M. P.; Que, E. L.; Que, L. *J. Am. Chem. Soc.* **2003**, *125*, 2113.
- (16) Lee, D.; Lippard, S. J. *Inorg. Chem.* **2002**, *41*, 827.
- (17) Tshuva, E. Y.; Lee, D.; Bu, W. M.; Lippard, S. J. *J. Am. Chem. Soc.* **2002**, *124*, 2416.
- (18) Kuzelka, J.; Farrell, J. R.; Lippard, S. J. *Inorg. Chem.* **2003**, *42*, 8652.
- (19) Du Bois, J.; Mizoguchi, T. J.; Lippard, S. J. *Coord. Chem. Rev.* **2000**, *200*, 443.
- (20) Herold, S.; Lippard, S. J. *J. Am. Chem. Soc.* **1997**, *119*, 145.
- (21) Tshuva, E. Y.; Lippard, S. J. *Chem. Rev.* **2004**, *104*, 987.
- (22) Kim, J.; Harrison, R. G.; Kim, C.; Que, L. *J. Am. Chem. Soc.* **1996**, *118*, 4373.
- (23) Que, L.; Tolman, W. B. *Angew. Chem., Int. Ed.* **2002**, *41*, 1114.
- (24) Feig, A. L.; Masschelein, A.; Bakac, A.; Lippard, S. J. *J. Am. Chem. Soc.* **1997**, *119*, 334.
- (25) Hagadorn, J. R.; Que, L.; Tolman, W. B. *J. Am. Chem. Soc.* **1998**, *120*, 13531.

\* E-mail: Gerhard.PIRNGRUBER@ifp.fr. Tel +33 4 78 02 27 33. Fax +33 4 78 02 20 66.

<sup>†</sup> Current address: Department of Catalysis and Separation, Institut Français du Pétrole, F-69390 Vernaison, France.

(1) Kitajima, N.; Ito, M.; Fukui, H.; Morooka, Y. *J. Chem. Soc., Chem. Commun.* **1991**, 102.

substratum and the oxidant are soluble. Most of the early generation model complexes activated the substrate via free radicals.<sup>26</sup> More recently, however, several high-valence iron-oxo complexes have been identified, which directly activate and oxidize the substrate, thereby truly mimicking the catalytic function of the enzyme.<sup>27–29</sup>

Although the active core of the enzyme is crucial for its catalytic function, one should be aware that the remainder of the enzyme (MMO has a molecular weight of 300 kDa) is not superfluous, but plays an important role in assembling the amino acid ligands around the metal core as well as in forming a specific binding pocket for the substrate (for coenzymes and regulators involved in the catalyzed reaction). Noncovalent interactions (H-bonding, electrostatic interactions, and van der Waals interactions) between the substrate and the amino acid residues adsorb the substrate in the binding pocket. The fact that the three metalloproteins MMO, ribonucleotide reductase (RNR-R2), and fatty acid desaturase ( $\Delta$ -9 ACP) have very similar diiron cores but entirely different catalytic functions confirms the importance of the more distant environment of the active site.

The absence of such a binding site in the above-mentioned inorganic model compounds is one of their major limitations. In the hydroxylation of alkanes, the substrate is hydrophobic, whereas the metal complex is hydrophilic and has little affinity for the substrate. An interesting approach to overcome that limitation is to carry out the reaction in micellar systems, where an inorganic iron complex is occluded in the hydrophobic core of the micelle.<sup>3,30</sup> Even better results are obtained when the complex is embedded in a hydrophobic layer on a silica support.<sup>31</sup> The hydrophobic layer approximates the binding pocket of the enzyme. Also encapsulation in polydimethylsiloxane membrane has been used.<sup>32</sup> With these systems, oxidation reactions can be carried out in aqueous solution instead of using organic solvents.

One can, however, go much further in trying to copy the hydrophobic binding site of the natural enzyme: State of the art methods in protein science make it possible to design a full-fledged protein that mimics the function of MMO. As a first step, the amino acid sequence of the natural enzyme is analyzed to identify the parts that are decisive for the binding of the metal core and the formation of hydrophobic pocket.<sup>33</sup> Short peptides are then synthesized that contain these crucial structural features and can, therefore, self-assemble with metal ions to manmade metalloproteins. Using such a retro structural analysis in combination with computational design, we could prepare realistic imitations of natural enzymes were prepared.<sup>34</sup> This approach helps us

understand the role of the amino acid sequence in the formation of the active site, but it remains difficult to combine a high accessibility of the active site with a stable protein folding.<sup>35</sup>

We chose a strategy for the synthesis of MMO mimics that is midway between the two approaches described above, i.e., between metal organic model complexes and “de novo” designed proteins. We did not want to use complex, synthetic ligands, but amino acids. In contrast to designed proteins, however, we used only a short peptide chain, i.e., the sequence His-Gly-Gly-Glu, which is found in the active core of MMO. The peptide chain was immobilized on a mesoporous silica support and complexes with iron and copper were formed by self-assembly with the immobilized ligands. The immobilization on a porous support fulfills several functions: (1) the concave pore brings the amino acid residues in close vicinity, as does the folding of the peptide in the natural enzyme or in “de novo” designed proteins. This should be favorable for the self-assembly of complexes with the metal ions. (2) Problems of solubility of the complex are circumvented and dimerization is prohibited. (3) It is possible to generate a hydrophobic environment in the pore, in order to favor the adsorption of the hydrophobic substrates. The present contribution is a continuation of earlier work in which only single amino acids were immobilized.<sup>36</sup>

## Experimental Section

**Supports.** Mesoporous silica was synthesized according to a literature procedure.<sup>37,38</sup> A purely siliceous material with a surface area of 940 m<sup>2</sup> g<sup>-1</sup>, a pore volume of 2.2 cm<sup>3</sup> g<sup>-1</sup>, and an average pore diameter of 7 nm was obtained. The surface of the silica was functionalized with randomly distributed methyl- and aminopropyl groups by cografting of methyltrimethoxysilane and aminopropyltrimethoxysilane.<sup>39</sup> This support is labeled Supp\_isol. A silica material functionalized with methyl groups and pairs of aminopropyl groups was obtained by using the more complex 4,4'-bis[*N*-(3-trimethoxysilylpropyl)formimidoyl]benzene molecule and methyltrimethoxysilane as grafting agents. The distance between the amino groups of a pair is approximately 7 Å.<sup>40,41</sup> This support is labeled Supp\_pair. Detailed procedures for the synthesis of the mesoporous silica support and its functionalization can be found in the Supporting Information.

**Coupling of GlyHis(Trt)GlyGlyGlu(O<sup>t</sup>Bu)boc (A) to a Support.** The synthesis of the fully protected peptide GlyHis(Trt)GlyGlyGlu(O<sup>t</sup>Bu)boc (A) is described in the Supporting Information. A standard HBTU/HOBt/DMF activation procedure was used for the coupling of peptide A to amino-functionalized supports (HBTU, 2-(1H-benzotriazole-1-yl)-1,1,3,3-tetramethyluronium hexafluorophosphate; HOBt, *N*-hydroxybenzotriazole). A (120 mg, 0.14

(26) MacFaul, P. A.; Ingold, K. U.; Wayner, D. D. M.; Que, L. *J. Am. Chem. Soc.* **1997**, *119*, 10594.

(27) Costas, M.; Mehn, M. P.; Jensen, M. P.; Que, L. *Chem. Rev.* **2004**, *104*, 939.

(28) Shan, X. P.; Que, L. *J. Inorg. Biochem.* **2006**, *100*, 421.

(29) Foster, T. L.; Caradonna, J. P. *J. Am. Chem. Soc.* **2003**, *125*, 3678.

(30) Prieto, T.; Nascimento, O. R.; Tersariol, I. L. S.; Faljoni-Alario, A.; Nantes, I. L. *J. Phys. Chem. B* **2004**, *108*, 11124.

(31) Neimann, K.; Neumam, R.; Rabion, A.; Buchanan, R. M.; Fish, R. H. *Inorg. Chem.* **1999**, *38*, 3575.

(32) Parton, R. F.; Vankelecom, I. F. J.; Casselman, M. J. A.; Bezoukhanova, C. P.; Uytterhoeven, J. B.; Jacobs, P. A. *Nature* **1994**, *370*, 541.

(33) Lombardi, A.; Summa, C. M.; Geremia, S.; Randaccio, L.; Pavone, V.; DeGrado, W. F. *Proc. Natl. Acad. Sci. U.S.A.* **2000**, *97*, 6298.

(34) Summa, C. M.; Rosenblatt, M. M.; Hong, J. K.; Lear, J. D.; De Grado, W. F. *J. Mol. Biol.* **2002**, *321*, 923.

(35) Di Costanzo, L.; Wade, H.; Geremia, S.; Randaccio, L.; Pavone, V.; DeGrado, W. F.; Lombardi, A. *J. Am. Chem. Soc.* **2001**, *123*, 12749.

(36) Luechinger, M.; Kienhofer, A.; Pirngruber, G. D. *Chem. Mater.* **2006**, *18*, 1330.

(37) Lindlar, B.; Kogelbauer, A.; Kooyman, P. J.; Prins, R. *Microporous Mesoporous Mater.* **2001**, *44*, 89.

(38) Luechinger, M.; Pirngruber, G. D.; Lindlar, B.; Laggner, P.; Prins, R. *Microporous Mesoporous Mater.* **2005**, *79*, 41.

(39) Luechinger, M.; Prins, R.; Pirngruber, G. D. *Microporous Mesoporous Mater.* **2005**, *85*, 111.

(40) Wulff, G.; Heide, B.; Helfmeier, G. *J. Am. Chem. Soc.* **1986**, *108*, 1089.

(41) Wulff, G.; Heide, B.; Helfmeier, G. *React. Polym.* **1987**, *6*, 299.

mmol) was dissolved together with HBTU (52.9 mg, 0.14 mmol) and HOBt (18.6 mg, 0.14 mmol) in DMF (2 mL). After 5 min, diisopropylethylamine (DIPEA) (24  $\mu$ L, 0.28 mmol) was added. Two hundred milligrams of amino-functionalized support (0.6 mmol amino groups per gram of support) was added to this solution and the resulting suspension was shaken for 60 min at room temperature. Filtration, washing with DMF, and drying under reduced pressure at 40 °C gave the peptide-modified material.

Side chain protecting groups (His(Trt) and Glu(O<sup>t</sup>Bu)) and the N-terminal boc protecting group of the immobilized peptides were removed by trifluoroacetic acid (TFA) treatment. Two hundred milligrams of the peptide-modified solid was added to a mixture containing TFA (4 mL), water (200  $\mu$ L), and triisopropylsilane (TIPS) (40  $\mu$ L). After being shaken at room temperature for 30 min, the solid was collected by filtration and washed with TFA and DCM. The solid was then suspended in a solution of pyridine (20% by volume) in ethanol. After 15 min of being shaken at room temperature, the solid was collected by filtration and washed with ethanol. The treatment was repeated 5 times, followed by two additional washings in pure ethanol. The resulting solid was dried under reduced pressure at 40 °C. The obtained materials are labeled as PepA\_X (X designates the support).

**Manual Synthesis of HisGlyGlyGlu on a Support.** Standard HBTU/HOBt/DMF coupling procedures for fmoc chemistry were applied for the synthesis of HisGlyGlyGlu on the amino-functionalized support. Fmoc-His(Trt), fmoc-Gly, and boc-Glu(O<sup>t</sup>Bu) were used. Fmoc-His(Trt) (1 mmol) was dissolved together with HBTU (1 mmol) and HOBt (1 mmol) in DMF (10 mL). DIPEA (2 mmol) was added and the solution kept for 30 s in an ultrasonic bath. One gram of the amino-functionalized support (0.6 mmol amino groups per gram of support) was suspended in this solution. The suspension was shaken at room temperature for 60 min. Then the solid was filtered, washed three times with DMF (5 mL), and dried under reduced pressure. To couple as much amino acid as possible, the coupling step was performed twice. After coupling of the first amino acid, residual amino groups were capped with acetic anhydride (see the Supporting Information). Cleavage of the fmoc protecting group was done by treatment of the functionalized support with piperidine in DMF. One gram of the functionalized support was shaken for 3 min in 7 mL of 2:8 piperidine:DMF. After filtration, this procedure was repeated four times. After the last filtration, the solid was washed three times with DMF (5 mL) and dried under reduced pressure. Two coupling steps with fmoc-Gly were then applied, the fmoc protecting group was cleaved, and another two fmoc-Gly coupling steps were carried out. After fmoc deprotection, two coupling steps with boc-Glu(O<sup>t</sup>Bu) were applied. The final His-(Trt)GlyGlyGlu(O<sup>t</sup>Bu)boc-modified material was dried under reduced pressure. Cleavage of the protecting groups (Trt, O<sup>t</sup>Bu, and boc) was carried out as described above. The obtained materials are labeled PepM\_X (X designates the support).

**Complexation.** Fe(II) acetate and Cu(II) acetate were used as metal sources for the complexations. Two hundred milligrams of functionalized support were suspended in 15 mL of a 0.1 M acetate buffer (pH 6.8). This suspension was degassed for 20 min with nitrogen. The metal salt (0.86 mmol) was added under nitrogen flow and the resulting suspension was stirred for 60 min at room temperature. After filtration, the materials were washed three times with acetate buffer (5 mL) and three times with ethanol (5 mL). Drying under reduced pressure gave the final metal complex functionalized materials.

**Characterization.** Nitrogen adsorption measurements were performed at liquid nitrogen temperature with a Tristar 3000 apparatus of Micromeritics. Prior to the measurements, the samples were degassed for at least 4 h at 10 Pa at 100 °C. IR spectra of the

materials were recorded in the range of 4000–1000  $\text{cm}^{-1}$ . The sample ( $\sim$ 2 mg) was pressed in a self-supporting pellet and treated at 200 °C for 1 h in a flow of He ( $\sim$ 25 mL/min) before the spectra were recorded at 100 °C. The spectrum of the empty cell was used as background. Normalization was done using the intensities of the overtone bands of the Si–O–Si lattice vibrations at 1874 and 1990  $\text{cm}^{-1}$ . The Fe and Cu content were determined by AAS, after dissolution of the samples in an HF/water/HNO<sub>3</sub> matrix over night. Organic elementary analysis (C, H, N) was performed on a LECO CHN-900 apparatus. Diffuse reflectance UV–vis spectra of the Fe- and Cu-exchanged materials were measured on a Cary 400 UV–vis spectrometer equipped with a praying mantis sample stage from Harrick. BaSO<sub>4</sub> was used as reference. EXAFS spectra at the Fe and Cu K-edge were measured at the Swiss–Norwegian Beamline at the ESRF in Grenoble. The beamline uses a Si(111) crystal for monochromizing the X-rays and a Cr mirror to reject harmonics and other high-order reflections. Spectra were collected in fluorescence mode, using a 13-element solid-state Ge detector. EXAFS analysis was carried out using the IFEFFIT software package.<sup>42</sup> X-band CW EPR (microwave (mw) frequency 9.5 GHz) measurements were carried out in powder form on a Bruker E500 spectrometer equipped with a liquid nitrogen cryostat at 120 K. A modulation amplitude of 0.2 mT, a modulation frequency of 100 kHz, and a microwave power of 6.37 mW (15 dB) were used.

**Catalytic Tests.** All materials were tested as catalysts for cyclohexane oxidation. Hydrogen peroxide (H<sub>2</sub>O<sub>2</sub>) was used as oxidant. The oxidation reactions were carried out in 10 mL glass flasks. Four milliliters of acetonitrile was placed in the flask and degassed with nitrogen for 5 min. Next, 1000  $\mu$ mol of cyclohexane and 200  $\mu$ mol of H<sub>2</sub>O<sub>2</sub> (30% in water) were added. The reaction was started by adding 50 mg of catalyst. After addition of the catalyst, the reaction mixture was further degassed for 30 s to remove oxygen. The reaction mixture was stirred at 30 °C in an oil bath. Samples (0.25 mL) were taken after certain periods from the reaction and analyzed by gas chromatography (HP 5890 Series II, HP-1 column with FID detector and HP5890 Series II, DB-17 column with FID detector). 1-Pentanol was used as internal standard for the quantification.

## Results

We followed two different strategies to immobilize the short peptide on the silica support: In the first method, a peptide that was prepared on a solid-phase peptide synthesizer (SPPS) was coupled to an amino-functionalized support. A similar method has been successfully applied to carbon nanotubes.<sup>43,44</sup> In the second method, the peptide was synthesized directly on the amino-functionalized silica support.

**Coupling of a SPPS-Prepared Peptide to the Support.** Scheme 1 schematically shows the immobilization of Gly-HisGlyGlyGlu on the amino-functionalized supports. The key step is the coupling of the SPPS-prepared peptide with the silica material by reaction of the nucleophilic surface amino groups with the activated electrophilic C-terminal carboxyl group of the peptide. We used a standard activation/coupling

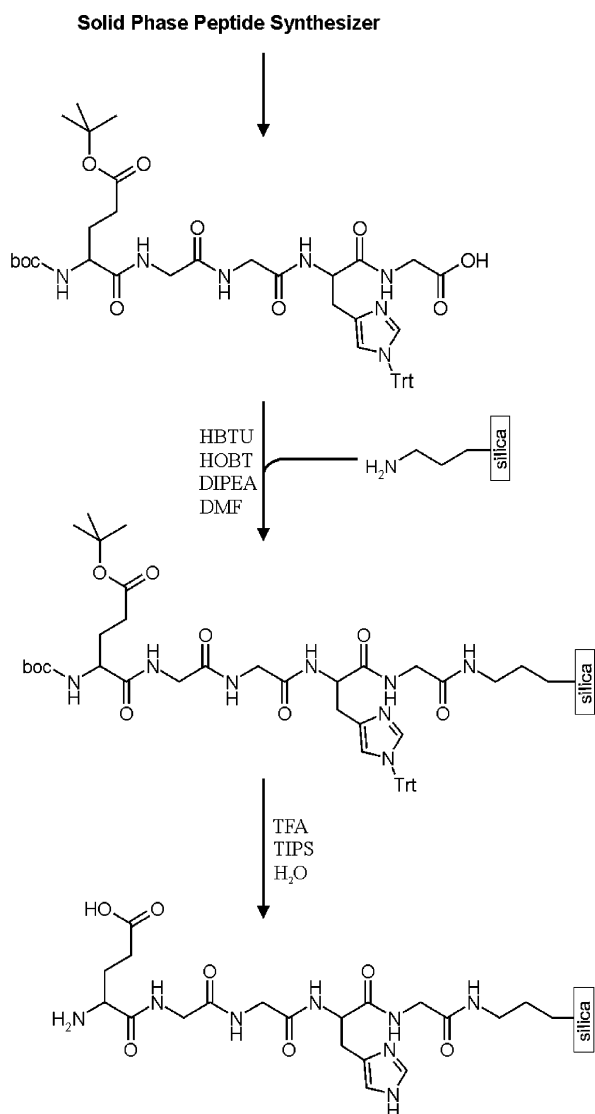
(42) Newville, M. *J. Synchrotron Radiat.* **2001**, *8*, 322.

(43) Georgakilas, V.; Tagmatarchis, N.; Pantarotto, D.; Bianco, A.; Briand, J. P.; Prato, M. *Chem. Commun.* **2002**, 3050.

(44) Pantarotto, D.; Partidos, C. D.; Graff, R.; Hoebeke, J.; Briand, J. P.; Prato, M.; Bianco, A. *J. Am. Chem. Soc.* **2003**, *125*, 6160.



**Scheme 1. Immobilization of the Fully Protected Peptide GlyHisGlyGlyGlu on Amino-Functionalized Silica by Coupling of the SPPS-Prepared Peptide; For Abbreviations, See Scheme 2**



method with HOBT and HBTU as coupling reagents.<sup>45</sup> To avoid undesired side reactions, the peptide was protected on all reactive groups except the C-terminal carboxyl group. The chosen protecting groups (boc, O<sup>t</sup>Bu, and Trt) could all be cleaved by TFA, which allows full deprotection in one single step.<sup>46</sup> The chosen protective groups are compatible with standard fmoc chemistry, so that the peptide could be synthesized on a solid-phase peptide synthesizer (SPPS) using standard procedures. An acid-labile resin (2-chlorotrityl) was used for the peptide synthesis, which allowed cleavage of the peptide from the resin under mild conditions without removing the protecting groups. The obtained product after solid-phase peptide synthesis was purified by HPLC. The major product (95% w/w) corresponded to the fully protected peptide (ESI-MS: 854 Da). The other

(45) White, P. D.; Dörner, B.; Steinauer, R. *Novabiochem Catalog 2002/2003—Synthesis Notes*; Novabiochem: Laufelfingen, Switzerland, 2003.

(46) Greene, T. W.; Wuts, P. G. M. *Protective Groups in Organic Synthesis*; John Wiley & Sons: New York, 1999.

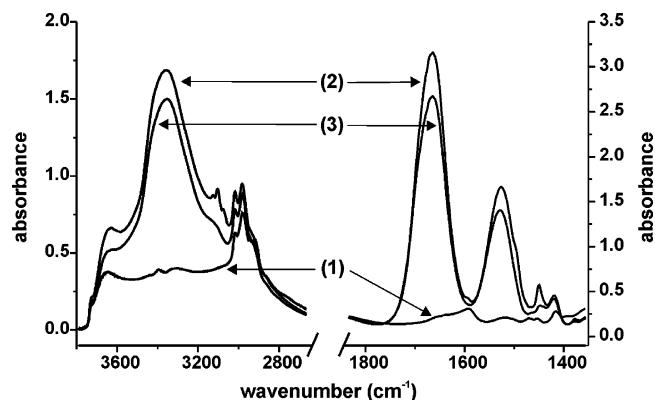


**Figure 1.** IR spectra of amino-functionalized silica (1) before coupling of the peptide GlyHis(Trt)GlyGlyGlu(O<sup>t</sup>Bu)boc, (2) after coupling, and (3) after deprotection.

products were fragments or partly deprotected peptide. The purified peptide was used for coupling with the support.

The coupling of the peptide could be followed by IR. Figure 1 shows the IR spectra of the amino-functionalized support before and after coupling of the peptide. The spectrum before coupling shows two main features: the bands around 2900 cm<sup>-1</sup> are due to symmetric and asymmetric CH<sub>2</sub> and CH<sub>3</sub> stretching vibrations of the aminopropyl and methyl groups. The band at 1595 cm<sup>-1</sup> is an NH deformation vibration of the free amine groups.<sup>47</sup> After coupling of the peptide, the NH band decreases and the two characteristic bands for amide groups appear at 1670 and 1550 cm<sup>-1</sup>. The bands observed for the amide groups are caused by the newly formed amide bond, but also by the amide bonds present in the peptide. The bands at 3060 cm<sup>-1</sup> are caused by CH vibrations of the triphenylmethyl protecting group. The broad feature above 3100 cm<sup>-1</sup> is due to vibrations of the NH bond in amides and is typical for amino acids.<sup>47</sup> Many possible H bonds in the peptide contribute to the broadness of this feature.

The GlyHis(Trt)GlyGlyGlu(O<sup>t</sup>Bu)boc-modified M41S was subjected to a deprotection step with TFA (Scheme 1). Removal of the boc protecting group results in the removal of one amide bond (Figure 1). This is reflected in the decrease in the amide bands (1670 and 1559 cm<sup>-1</sup>). The disappearance of the bands at 3060 cm<sup>-1</sup> shows the cleavage of the Trt protecting group. The cleavage of the *tert*-butyl protecting group on the glutamic acid side chain could not be observed because the carbonyl band of the ester group is hidden below the amide band.

The surface area as well as pore volume of the amino-functionalized silica supports decreased upon coupling of the peptide and increased slightly after deprotection of the bulky protecting groups (see Table S1 in the Supporting Information). The loading of the support with peptide was calculated after subtraction of the contribution of the anchoring groups on the support (see Table 1). The GlyHisGlyGlyGlu peptide sequence has a 17:7 carbon:nitrogen ratio, or 2.43. The C<sub>pep</sub>/N<sub>pep</sub> ratios of the SPPS-prepared peptide-modified materials are very close to the theoretical value of the sequence. This shows that a very uniform modification with GlyHisGly-

(47) Colthup, N. B.; Daly, L. H.; Wiberley, S. E. *Introduction to Infrared and Raman Spectroscopy*; Academic Press: London, 1990.

**Table 1. Organic Loadings of Supports and Peptide-Modified Materials**

sample	$C_{\text{tot}}^a$ (mmol g <sup>-1</sup> )	$N_{\text{tot}}^b$	$C_{\text{pep}}^c$ (mmol g <sup>-1</sup> )	$N_{\text{pep}}^d$	Pep <sup>e</sup> (mmol g <sup>-1</sup> )	$C_{\text{pep}}/N_{\text{pep}}$
Supp_pair	3.3	0.6				
Supp_isol	4.7	0.9				
PepA_pair	7.1	2.1	3.8	1.5	0.22	2.5
PepA_isol	7.5	2.0	2.8	1.1	0.16	2.5
PepM_pair	10.8	2.6	7.5	2	0.33 <sup>f</sup>	3.7
PepM_isol	12.1	2.9	7.4	2	0.35 <sup>f</sup>	3.5

<sup>a</sup> Total amount of carbon ( $\pm 3\%$ ). <sup>b</sup> Total amount of nitrogen ( $\pm 3\%$ ). <sup>c</sup>  $C_{\text{pep}} = C_{\text{tot}}(\text{PepX}) - C_{\text{tot}}(\text{SuppX})$ . <sup>d</sup>  $N_{\text{pep}} = N_{\text{tot}}(\text{PepX}) - N_{\text{tot}}(\text{SuppX})$ . <sup>e</sup> For PepA, Pep =  $N_{\text{pep}}/7$ ; for PepM, Pep =  $N_{\text{pep}}/6$ . <sup>f</sup> Assuming exclusive formation of the desired sequence HisGlyGlyGlu.

GlyGlu was obtained. The amount of peptide can be calculated as  $N_{\text{pep}}/7$  (seven nitrogen atoms in the sequence). 35% of the surface amino groups of Supp\_pair and 18% of Supp\_isol reacted with the peptide.

**Step-by-Step Synthesis of the Peptide Directly on the Functionalized Silica Supports.** In the step-by-step synthesis, the desired peptide is synthesized directly on the functionalized support by coupling one amino acid after the other. In principle, it is possible to use a SPPS to couple amino acids to an amino-functionalized support.<sup>36</sup> Because the automated synthesis has practical limitations in terms of the amount of sample that can be handled (less than 250 mg of support material in our case), we preferred not to use the SPPS for our step-by-step synthesis, but performed the synthesis manually, following exactly the same chemical protocols as those used by an automated peptide synthesizer (Scheme 2).

The step-by-step synthesis strategy has a fundamental drawback. Incomplete coupling steps lead to the formation of fragments of the desired peptide, which cannot be removed in an HPLC purification step, as after the SPPS synthesis. To avoid such formation of unwanted fragments, we used an excess of amino acid for the coupling. All coupling steps were repeated twice before the next amino acid was added. Moreover, after coupling of the first amino acid, unreacted amino groups were capped by reaction with acetic anhydride. This measure prevented the surface amino groups from starting a new peptide chain upon coupling of the next amino acid.

Figure 2 shows the IR spectra of the materials obtained after each coupling step. We observed a stepwise increase of intensity of the broad feature above 3100 cm<sup>-1</sup>, which is caused by vibrations of the NH bond in amides (typical for amino acids)<sup>47</sup> and by H-bond interactions in the growing peptide. Three bands at 3060 cm<sup>-1</sup>, showing the presence of CH bonds of aromatic systems (Trt and fmoc protecting groups), are found after coupling of fmocHis(Trt). The characteristic amide bands show a stepwise increase in intensity. A significant broadening of the 1670 cm<sup>-1</sup> band is observed after coupling of Glu(O<sup>t</sup>Bu)boc because of the incorporation of an ester group in the side chain of the amino acid. The protecting groups were removed by treatment with TFA, which could be followed by IR (spectra not shown).

Surface area and pore volume of the support decreased because of the formation of a layer of peptide on the pore surface (see Table S1 in the Supporting Information). The peptide loading was calculated from the organic analysis as before (see Table 1). The HisGlyGlyGlu sequence has a carbon to nitrogen ratio of 15:6 = 2.5. The  $C_{\text{pep}}/N_{\text{pep}}$  ratios of the step-by-step peptide-modified materials are somewhat

higher. This indicates that some sequences with higher C/N ratios were formed along with HisGlyGlyGlu. The C/N ratios of the three amino acids Gly, His and Glu are 2, 2, and 5, i.e., there should be an excess of Glu compared to His and Gly. We infer that some incomplete GlyGlyGlu sequences were formed along with HisGlyGlyGlu (in spite of the capping of unreacted surface amino groups by acetic anhydride). For the estimation of the amount of immobilized peptide, we ignored the formation of incomplete sequences and used the formula  $N_{\text{pep}}/6$ . The thus-calculated peptide loadings are significantly higher than for the SPPS-prepared peptide-modified materials described in the previous section. Repeating all coupling steps twice in the manual step-by-step synthesis allowed us to immobilize more peptide on the support.

**Complexation of Metal Ions.** To form the complexes of the amino acids and the metals, the four support materials were suspended in a solution of Cu<sup>2+</sup> acetate or Fe<sup>2+</sup> acetate in an acetate buffer (pH 6.8). The amino-functionalized supports (without peptide) were also subjected to the same treatment. A buffer was used to compensate acidic protons from the supported peptide. Acetate salts and acetate buffer were chosen because acetate serves as bridging ligand between the iron atoms in MMO.<sup>21,48</sup> Moreover, acetate may also serve as a terminal ligand, if required (replacing missing glutamic acid groups). At pH 6.8, most of the imidazole rings of the histidine side chain ( $pK_a = 6.00$ ) as well as the carboxylic acid in the side chain of glutamic acid ( $pK_a 4.25$ ) are deprotonated and thus available for a possible complexation.<sup>49–52</sup> A higher pH should be avoided in order to prevent the formation of insoluble hydroxides of iron or copper.

We obtained iron loadings ranging from 0.13 to 0.17 mmol/g and Cu loadings ranging from 0.01 to 0.09 mmol/g (Table 2). In the case of Cu, the loading strongly increased from the support materials without peptide to the SPPS peptide and to the manually synthesized peptide. The iron loading was much less sensitive to the nature of the support. Iron has a broad ligand spectrum (His, Glu, Asp, Tyr, and Cys)<sup>53</sup> and can form complexes with amino groups of the

(48) Rosenzweig, A. C.; Frederick, C. A.; Lippard, S. J.; Nordlund, P. *Nature* **1993**, *366*, 537.

(49) Mesu, J. G.; Visser, T.; Soulimani, F.; van Faassen, E. E.; de Peinder, P.; Beale, A. M.; Weckhuysen, B. M. *Inorg. Chem.* **2006**, *45*, 1960.

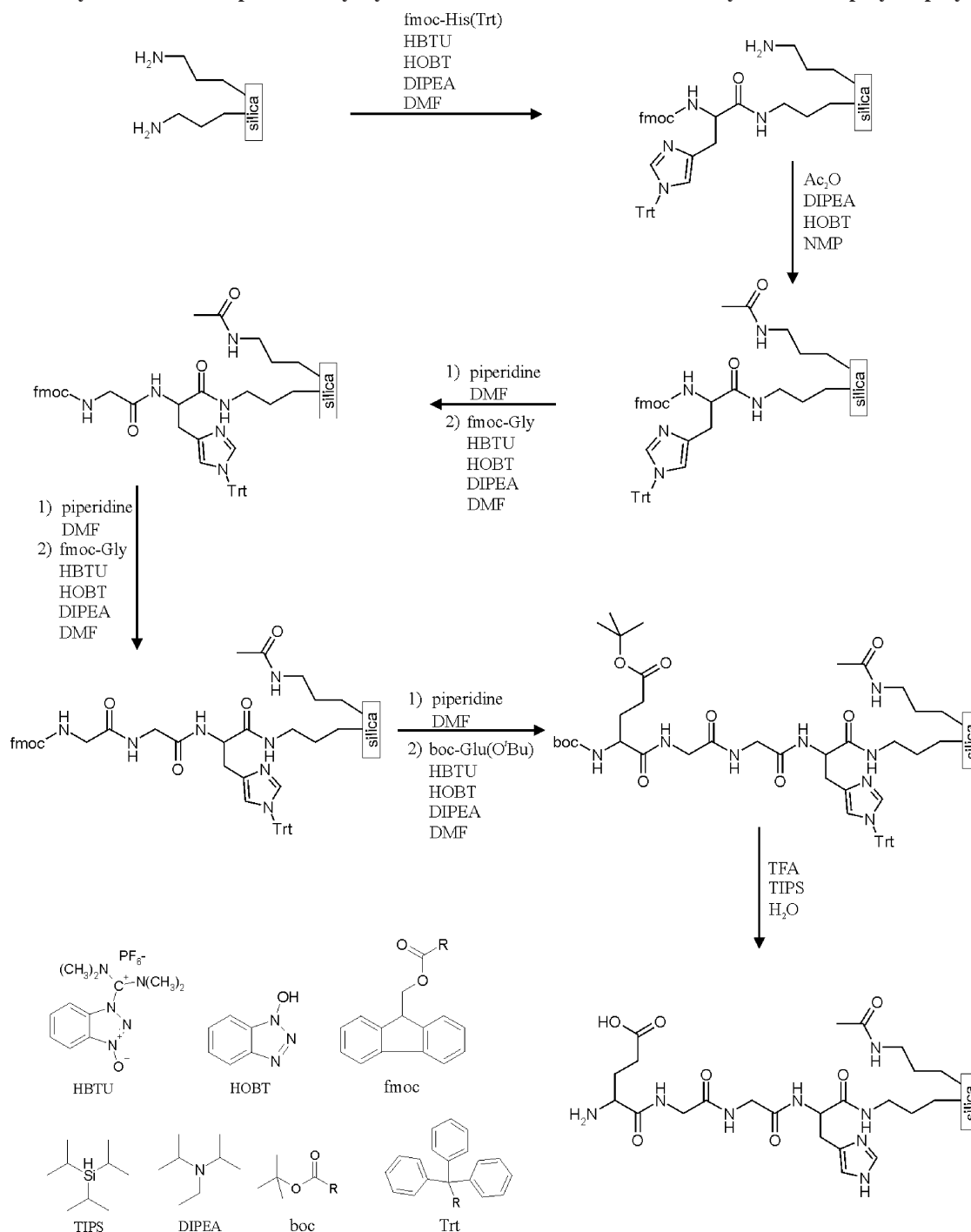
(50) Grommen, R.; Manikandan, P.; Gao, Y.; Shane, T.; Shane, J. J.; Schoonheydt, R. A.; Weckhuysen, B. M.; Goldfarb, D. *J. Am. Chem. Soc.* **2000**, *122*, 11488.

(51) Weckhuysen, B. M.; Verberckmoes, A. A.; Fu, L. J.; Schoonheydt, R. A. *J. Phys. Chem.* **1996**, *100*, 9456.

(52) Weckhuysen, B. M.; Verberckmoes, A. A.; Vannijvel, I. P.; Pelgrims, J. A.; Buskens, P. L.; Jacobs, P. A.; Schoonheydt, R. A. *Angew. Chem., Int. Ed.* **1996**, *34*, 2652.

(53) Williams, R. J. P. *Pure Appl. Chem.* **1983**, *55*, 1089.

Scheme 2. Synthesis of the Peptide HisGlyGlyGlu on Amino-Functionalized Silica by Manual Step-by-Step Synthesis



support, whereas Cu strongly prefers complexation by His. Therefore, the Cu content is more strongly correlated with the peptide loading. Surface area and pore volume are not significantly influenced by complexation of the metal ions (Table 2 compared to Table S1).

**UV-vis.** None of the UV-vis spectra of the iron-exchanged samples (see Figure S1 in the Supporting Information) showed the typical bands of Fe(II) acetate (measured as a reference) or of clustered iron oxides (characterized by strong absorptions below 30 000 cm<sup>-1</sup>). LMCT transitions at 44 000 and 37 000 cm<sup>-1</sup> indicate the formation of complexes between iron and amino acid residues for the peptide-modified materials or between iron and amino groups for the support materials. Because no d-d

transitions could be detected below 20 000 cm<sup>-1</sup> (the d-d transitions are spin- and Laporte-forbidden and therefore very weak), no further conclusions about the structure and symmetry of these complexes could be drawn.

The UV-vis spectra of the Cu-peptide complexes show an LMCT band at 39 000 cm<sup>-1</sup> (Figure S2 in the Supporting Information), which is not present in Supp\_isol\_Cu. The band is caused by a LMCT between an amino acid residue and copper (i.e., His).<sup>54</sup> The positions of the d-d transition absorption bands (15 100 cm<sup>-1</sup>) are consistent with the values reported by Weckhuysen et al.<sup>49-52</sup> for Cu-His complexes

(54) Fawcett, T. G.; Bernarducci, E. E.; Kroghjerspersen, K.; Schugar, H. J. *J. Am. Chem. Soc.* **1980**, *102*, 2598.

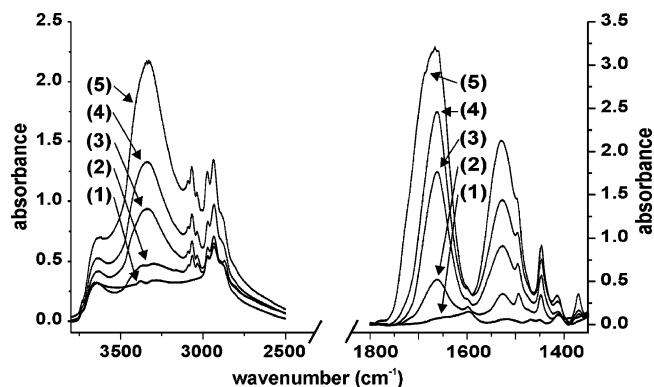


**Figure 2.** IR spectra obtained after each coupling step during the manual step-by-step synthesis of His(Trt)GlyGlyGlu(O<sup>t</sup>Bu)boc. (1) Support with isolated amino groups; (2) after coupling of fmocHis(Trt) (sequence His(Trt)fmoc); (3): after coupling of fmocGly (sequence His(Trt)Glyfmoc); (4) after coupling of fmocGly (sequence His(Trt)GlyGlyfmoc); (5) after coupling of bocGlu(O<sup>t</sup>Bu) (sequence His(Trt)GlyGlyGlu(O<sup>t</sup>Bu)boc).

with four nitrogen ligands in the equatorial plane (NNNN coordination) and two oxygen ligands in the axial positions.

**EPR.** The EPR spectra of the Cu complexes were recorded (see Figure S3 in the Supporting Information) in order to determine the number of nitrogen atoms in the first coordination shell of Cu via the hyperfine splitting pattern.<sup>49</sup> Unfortunately, the hyperfine splitting could not be resolved, which indicates that the complexes are not well-defined. A weak signal at half field indicates the presence of Cu dimers.

**EXAFS.** The EXAFS spectra of the metal–peptide complexes are clearly different from those of the metal-exchanged support materials (Figure 3). The peptide-modified materials have larger contributions at 2.2 and 3.4 Å. The maximum in the Fourier transform at 3.4 Å corresponds to a very long scattering path (>4 Å). This makes assignment to a Cu neighbor unlikely. Cu–Cu distances in dimers are usually not longer than 3.6 Å. The feature must therefore originate from the amino acid ligands. A relatively strong coherent backscattering from distant ligand atoms is possible only in a very rigid structure. A rigid structure element in our complexes is the imidazole ring of histidine. Indeed, the features at 2.2 and 3.4 Å could be rather well-fitted by single and multiple backscattering of imidazole, using a group fitting procedure.<sup>55</sup> This indicates that at least one of the ligands of Cu should be the imidazole ring of histidine. To refine the fits, other ligands had to be included in the model. In known complexes of Cu with amino acids<sup>56–61</sup> one usually finds four equatorial N or O ligands (amino groups, nitrogen atoms of the imidazole ring or carboxy groups) and two more distant axial ligands (carboxy groups or water). These

structural features were included in our fit models. The best fit was obtained with a structure containing two equatorial imidazole ligands, two additional equatorial N/O atoms, and two rather distant axial O atoms (see the Supporting Information for details). The EXAFS therefore indicates that one Cu atom is complexed by ligands from two peptide chains.

In the iron samples, a feature between 3 and 4 Å was also found, but it is less well-defined than for the Cu analogues. The signal-to-noise ratio of the iron spectra was significantly worse than of the Cu spectra, which affects the features at large distances in the Fourier transform. A fitting of the spectra was therefore not attempted. The XANES region indicates that the average oxidation state of the samples is close to Fe<sup>3+</sup>.

The EXAFS spectra of the metal-peptide complexes on Supp\_isol and on Supp\_pair were identical (see Figure S4 in the Supporting Information), i.e., there was no obvious difference in the coordination of the metal ions by paired or isolated peptide chains. The mode of synthesis (direct step-by-step or separate SPSS synthesis) also had no impact on the EXAFS spectra.

**Catalytic Tests.** As in numerous other studies on biomimetic complexes, the oxidation of cyclohexane was chosen as a test reaction. MMO uses O<sub>2</sub> + NADH as the oxidant. The chemical equivalent of O<sub>2</sub> + NADH is H<sub>2</sub>O<sub>2</sub>. H<sub>2</sub>O<sub>2</sub> is therefore a logical choice as the oxidant. It has the disadvantage, however, that H<sub>2</sub>O<sub>2</sub> can generate highly reactive and therefore rather unselective OH· radicals. Moreover, there are solubility problems between the aqueous H<sub>2</sub>O<sub>2</sub> solution and the substrate. Our reaction conditions are therefore certainly not optimized. The catalytic tests should be regarded as a comparative characterization method rather than a goal in its own.

Cyclohexanol (CyOL) and cyclohexanone (CyON) were the only products formed in the oxidation of cyclohexane (CyAN) with H<sub>2</sub>O<sub>2</sub> and our catalysts. No overoxidized products were observed. The iron-exchanged supports produced mainly CyON (Table 3). The turn over number (TON) as well as the total product yield of the iron–peptide complexes were higher than those of the Fe supports. Especially the TON of CyOL was significantly higher, resulting in higher CyOL: CyON ratios.

Similar trends were observed for the copper catalysts. The peptide complexes had higher TONs for CyOL than the Cu-support materials. Compared to iron, the TONs are generally higher, but the absolute product yields are lower, because of the lower metal loading. Cu<sup>2+</sup> is known to be more active in the oxidation of cyclohexyl radicals than Fe<sup>3+</sup>.<sup>62</sup>

In case of the metal-exchanged supports, about 10% of the metal leached during the reaction. The peptide-modified materials did not show any decrease in the metal content, i.e., there was no measurable leaching. To confirm this, we removed the catalyst by filtration after 2 h and continued

(55) Strange, R. W.; Blackburn, N. J.; Knowles, P. F.; Hasnain, S. S. J. *Am. Chem. Soc.* **1987**, *109*, 7157.

(56) Camerman, N.; Fawcett, J. K.; Kruck, T. P. A.; Sarkar, B.; Camerman, A. *J. Am. Chem. Soc.* **1978**, *100*, 2690.

(57) Purkayastha, P.; Sarma, B. K.; Talukdar, A. N. *Indian J. Pure Appl. Phys.* **2003**, *41*, 350.

(58) Yamauchi, O.; Odani, A.; Kohzuma, T.; Masuda, H.; Toriumi, K.; Saito, K. *Inorg. Chem.* **1989**, *28*, 4066.

(59) Masuda, H.; Odani, A.; Yamauchi, O. *Inorg. Chem.* **1989**, *28*, 624.

(60) Sasada, Y.; Takenaka, A.; Furuya, T. *Bull. Chem. Soc. Jpn.* **1983**, *56*, 1745.

(61) Ono, T.; Shimanouchi, H.; Sasada, Y.; Sakurai, T.; Yamauchi, O.; Nakahara, A. *Bull. Chem. Soc. Jpn.* **1979**, *52*, 2229.

(62) Sheldon, R. A.; Kochi, J. K. *Metal-Catalyzed Oxidations of Organic Compounds: Mechanistic Principles and Synthetic Methodology Including Biochemical Processes*; Academic Press: New York, 1981.

(63) van den Berg, T. A.; de Boer, J. W.; Browne, W. R.; Roelfes, G.; Feringa, B. L. *Chem. Commun.* **2004**, 2550.



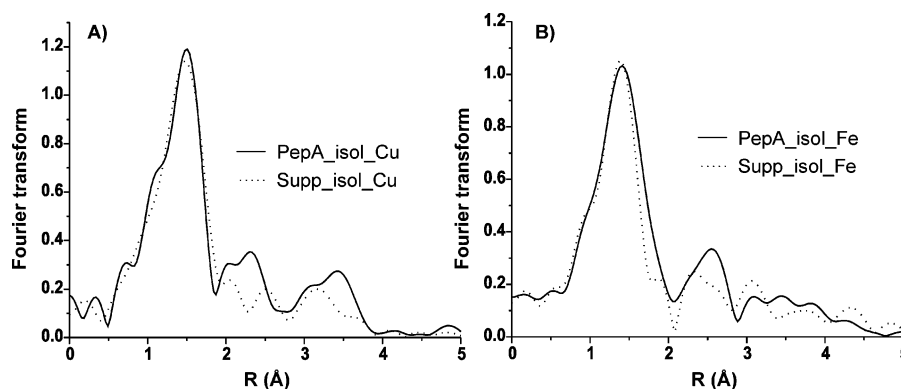


**Figure 3.** (A) Absolute part of the Fourier transforms of the Cu K edge EXAFS of the support material (dotted line) and of the peptide-modified material (solid line);  $k^2$  weighted,  $2.5 \text{ \AA}^{-1} < k < 11 \text{ \AA}^{-1}$ . (B) Absolute part of the Fourier transforms of the Fe K edge EXAFS of the support material (dotted line) and of the peptide-modified material (solid line);  $k^2$  weighted,  $2.5 \text{ \AA}^{-1} < k < 10.8 \text{ \AA}^{-1}$ .

**Table 2. Nitrogen Adsorption Data and Metal Loadings of the Samples after Complexation**

sample	metal loading <sup>a</sup> (wt %)	metal loading (mmol g <sup>-1</sup> )	surface area <sup>b</sup> (m <sup>2</sup> g <sup>-1</sup> )	pore volume <sup>b</sup> (cm <sup>3</sup> g <sup>-1</sup> )
PepM_pair_Fe	0.94	0.17	399	1.05
PepM_isol_Fe	0.89	0.16	406	1.07
PepA_pair_Fe	0.86	0.15	466	1.29
PepA_isol_Fe	0.81	0.14	411	1.12
Supp_isol_Fe	0.87	0.15	465	1.30
Supp_pair_Fe	0.77	0.13	491	1.38
PepM_pair_Cu	0.48	0.07	403	1.04
PepM_isol_Cu	0.55	0.09	412	1.03
PepA_pair_Cu	0.19	0.03	462	1.28
PepA_isol_Cu	0.14	0.02	406	1.10
Supp_isol_Cu	0.06	0.01	459	1.34
Supp_pair_Cu	0.02	0.01	506	1.42

<sup>a</sup> Error  $\pm$  5%. <sup>b</sup> Error  $\pm$  3%.

**Table 3. Data from Oxidation of Cyclohexane (1 mmol) with H<sub>2</sub>O<sub>2</sub> (0.2 mmol) and Different Catalysts (reaction time = 24 h)**

catalyst	total product <sup>a,b</sup> ( $\mu$ mol)	TON ( $\times 10^{-1}$ mol (mol metal) <sup>-1</sup> )		
		CyOL <sup>b</sup>	CyON <sup>b</sup>	CyOL:CyON
Supp_isol_Fe	2.3	0.7	2.9	0.2
Supp_pair_Fe	0.7	0.2	1	0.2
PepM_pair_Fe	3.7	2.2	2.6	0.8
PepM_isol_Fe	3.8	2.2	3.1	0.7
PepA_pair_Fe	2.7	1.4	2.4	0.6
PepA_isol_Fe	3.6	2.4	3	0.8
Supp_isol_Cu	0.3	0.8	6.2	0.1
Supp_pair_Cu	0.5	1.3	9.5	0.1
PepM_pair_Cu	2.8	1.7	6.5	0.3
PepM_isol_Cu	3.5	2.3	6.5	0.4
PepA_pair_Cu	1.5	4.1	7	0.6
PepA_isol_Cu	1.7	5.9	8.6	0.7

<sup>a</sup> Total amount of formed products:  $\mu$ mol CyOL +  $\mu$ mol CyON. <sup>b</sup> Error  $\pm$  10%.

the reaction. No conversion was observed after removal of the catalyst. The catalysts were reusable without significant loss of activity.

## Discussion

**Structure of the Metal–Peptide Complexes.** UV–vis and EXAFS show that the metal cations are complexed by the amino acids. The imidazole ring of histidine is part of the coordination sphere. The LMCT band in UV–vis at  $39\,000 \text{ cm}^{-1}$  can be assigned to a charge transfer from imidazole to copper.<sup>54</sup> When complexed only by histidine, copper prefers NNNN coordination in the equatorial plane and two carboxy ligands in the axial positions at pH 7 and NNNO coordination at pH 5.<sup>49</sup> Because our complexes were formed at pH = 6.8, a NNNN coordination is expected. The

UV–vis spectra of our materials confirm this (EXAFS cannot, unfortunately, distinguish between NNNO and NNNN). Two equatorial nitrogen atoms originate from the imidazole ring of His. The two other nitrogen atoms may be provided by the N-terminal free amino group and/or the nitrogen atoms of the amide bonds. Axial oxygen ligands are available from the carboxy group of Glu, from acetate ions, and from water. The fact that two imidazole rings are part of the coordination sphere of Cu indicates that Cu is complexed by ligands from two neighboring peptide chains. A structural model is proposed in Figure 4. The lack of hyperfine splitting in the EPR spectra of Cu and the presence of some Cu dimers show, however, that our samples do not contain a single well-defined species, but present mixtures of different coordination modes. We observed no difference



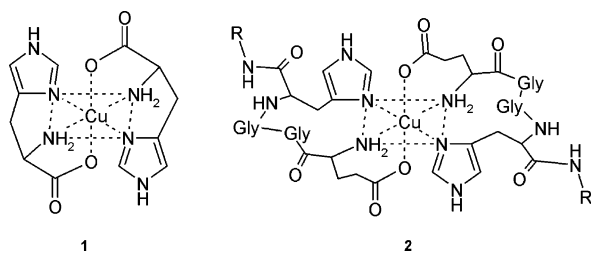


**Figure 4.** Analogy between the complex  $\text{Cu}(\text{His})_2$  (1) observed at pH 7 and a possible complex of Cu with HisGlyGlyGlu (2).<sup>49</sup>

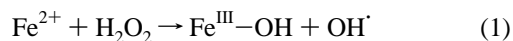
in the spectroscopic or catalytic properties between samples synthesized from paired amino supports and isolated amino supports. Length (eight bonds until the first imidazole ring on each peptide) and flexibility of the peptide are high enough to allow complexation of the metal ion with ligands from two peptides in both materials (see Scheme S1 in the Supporting Information). Likewise, the spectroscopic data and the catalytic results of the materials prepared by step-by-step coupling were very similar to those of the SPSS-prepared peptides. This validates the step-by-step coupling approach.

#### Self-Assembly vs Preassembly of the Metal Complexes.

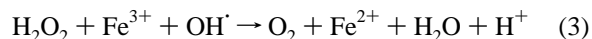
In our method, the metal-peptide complexes are formed by self-assembly with the immobilized ligands inside the pores of the support. The inherent disadvantage of the method is the almost inevitable formation of mixed coordination modes, i.e., the structures are badly defined. In contrast, well-defined immobilized metal–amino acid complexes can be obtained, for example, by ion exchange of preassembled complexes between Cu/Fe and amino acids into the zeolite faujasite.<sup>50–52</sup> The size of the complexes is limited by the diameter of the faujasite cage, i.e., 11.8 Å. Also, physical adsorption of preassembled complexes in mesoporous silica (MCM-41) has been used, but the complexes are susceptible to leaching.<sup>64,65</sup> In our method, the peptide ligands are covalently anchored to the support, which makes the structures very stable. The use of a mesoporous support allows the immobilization of long peptide chains. The complexes can be up to 70 Å in size. The synthesis of the peptide ligands according to the SPSS protocol is a reliable, highly flexible procedure that is amenable to high-throughput experimentation. In contrast to the methods described in refs 66 and 67, no dedicated synthesis of ligands or anchoring groups is required. These advantages weigh in against the inherent shortcoming of self-assembly mentioned above.

The use of a silica support with mesostructural order is probably not essential for the immobilization of the peptide. Commercial mesoporous silica is expected to behave similarly. However, the more uniform pore size distribution of our materials may be an advantage for the self-assembly, which is influenced by the confinement in the pore.

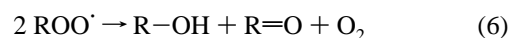
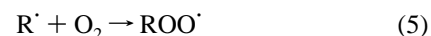
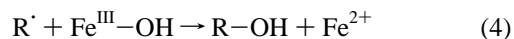
**Catalysis.** The oxidation of cyclohexane was used to compare the catalytic activity of the complexes. The product pattern observed in the oxidation with  $\text{H}_2\text{O}_2$  indicates that we are dealing with free radical chemistry. The initial step in the oxidation of CyAN by  $\text{H}_2\text{O}_2$  is the formation of  $\text{OH}^\cdot$  radicals according to eq 1.



The  $\text{OH}^\cdot$  radicals abstract a hydrogen atom from CyAN to form a cyclohexylradical  $\text{R}^\cdot$ . This reaction competes with the decomposition of  $\text{H}_2\text{O}_2$  by reaction 3.



The oxidation products CyOL and CyON can then be formed by two pathways: (a) a metal-based pathway where CyAN radicals react with  $\text{Fe}^{3+}\text{-OH}$  complexes to form CyOL and  $\text{Fe}^{2+}$  (eq 4) or (b) by autoxidation of CyAN radicals by  $\text{O}_2$  (originating from the parallel decomposition of  $\text{H}_2\text{O}_2$ ) forming CyOL and CyON (eqs 5 and 6).



In both pathways, CyOL can be further oxidized to CyON. Depending on the rate of the further oxidation of CyOL, high OL/ON ratios can be obtained in the metal-based pathway. In the autoxidation pathway CyOL and CyON are formed in a ratio of 1:1. Subsequent oxidation of CyOL to CyON will happen to the same extent as in the purely metal-based mechanism. One can therefore interpret an increase in the OL:ON ratio as an increase in metal-based oxidation over  $\text{H}_2\text{O}_2$  decomposition followed by autoxidation.

The observed OL:ON ratios were always smaller than one. Because of the long reaction times, the formed CyOL was further oxidized to CyON. All metal–peptide complexes had higher OL:ON ratios and higher total product yields than the metal–support materials. The peptide-modification favored direct metal-based oxidation via eq 4 vs autoxidation, which is, however, still dominating, and increased the overall activity. Also compared to our first generation biomimetic catalysts, constructed with single amino acids (histidine or glutamic acid) immobilized on a support,<sup>36</sup> the materials reported here have higher activities and selectivity to CyOL. The step from a single amino acid to the short peptide His-Gly-Gly-Glu leads to a clear improvement of the catalytic properties.

Compared to MMO,<sup>68,69</sup> the oxidation activity remains low (granting that our reaction conditions were not optimized). We partly attribute this to the failure to produce binuclear complexes in our materials. Binuclearity seems to be an essential feature of mono-oxygenases.<sup>28</sup> Also, the miscibility problems between oxidant and substrate may play a role. Lack of accessibility of the metal centers in our complexes should not be a reason for their lower reaction rate, because the axial oxygen ligands are rather labile.

(64) Hernadi, K.; Mehn, D.; Labadi, I.; Palinko, I.; Sitkei, E.; Kiricsi, I. *Stud. Surf. Sci. Catal.* **2002**, *142*, 85.

(65) Knops-Gerrits, P. P.; Verberckmoes, A.; Schoonheydt, R.; Ichikawa, M.; Jacobs, P. A. *Microporous Mesoporous Mater.* **1998**, *21*, 475.

(66) Walcarius, A.; Sayen, S.; Gérardin, C.; Hamdoune, F.; Rodehüser, L. *Colloids Surf., A* **2004**, *234*, 145.

(67) Blin, J. L.; Gérardin, C.; Rodehüser, L.; Selve, C.; Stébé, M. J. *Chem. Mater.* **2004**, *16*, 5071.

(68) Colby, J.; Stirling, D. I.; Dalton, H. *Biochem. J.* **1977**, *165*, 395.

(69) Stirling, D. I.; Colby, J.; Dalton, H. *Biochem. J.* **1979**, *177*, 361.

## Conclusions

We have described an inventive route for the synthesis of bioinspired metal–peptide complexes: The peptide sequence HisGlyGlyGlu (which is found in the active core of MMO) was coupled to an aminopropyl-modified mesoporous silica support by direct step-by-step coupling or by grafting of an SPPS-prepared purified peptide. Exposure of the immobilized peptides to iron or copper salt solution led to the self-assembly of stable metal–peptide complexes. EXAFS and UV–vis show that the imidazole ring of histidine is part of ligand sphere in all metal–peptide complexes. Two histidine moieties from two neighboring peptide chains coordinate to Cu. The other ligands of Cu are amide or amino groups of the peptide chain and axial carboxy groups or water. Compared to other methods of metal–peptide immobilization, the significant advance of our route is its simplicity and high versatility. The step-by-step peptide synthesis is especially suited for a high-throughput experimentation approach.<sup>70</sup>

In terms of catalytic activity, the complexes of iron and copper with the HisGlyGlyGlu peptide sequence are clearly superior to the iron or copper complexes with the non-peptide-modified support material and the first-generation

complexes with one single amino acid. This result proves the validity of our approach. Yet, numerous improvements are necessary.

Our complexes do not truly mimic the catalytic function of MMO, because they operate partly via free radicals and have a much lower activity.

Synthetic MMO mimics have binuclear iron or copper cores, whereas our complexes are essentially mononuclear. In view of the difficulty to prepare well-defined binuclear complexes by self-assembly, enzymes with mononuclear metal cores (for example, Rieske dioxygenases<sup>71</sup> or galactose oxidase,<sup>72</sup> both containing the 2-His-1-carboxylate facial triad) seem to be more realistic targets for future studies.

**Acknowledgment.** Dr. W. van Beek and Dr. H. Emmerich from the Swiss–Norwegian Beamline at ESRF Grenoble are acknowledged for their assistance in the EXAFS measurements. We thank Mr. Sreekanth Anandaram for the EPR measurements.

**Supporting Information Available:** Experimental details of the peptide synthesis, and additional characterization results (UV–vis, elemental analysis, surface area and pore volume analysis, EPR, and EXAFS) (PDF). This material is available free of charge via the Internet at <http://pubs.acs.org>.

CM070686V

(71) Oldenburg, P. D.; Que, L. *Catal. Today* **2006**, *117*, 15.

(72) Kervinen, K.; Bruijninx, P. C. A.; Beale, A. M.; Mesu, J. G.; van Koten, G.; Gebbink, R.; Weckhuysen, B. M. *J. Am. Chem. Soc.* **2006**, *128*, 3208.

(70) Jandeleit, B.; Schaefer, D. J.; Powers, T. S.; Turner, H. W.; Weinberg, W. H. *Angew. Chem., Int. Ed.* **1999**, *38*, 2495.